Fırat Üniversitesi Fen Bil. Dergisi
36(2), 59-66, 2024

Araştırma Makalesi

Martensitic Transformation Thermodynamic and Structure Analysis of CuAlFe High-Temperature Shape Memory Alloy

Oktay KARADUMAN[1], İskender ÖZKUL[2], Yakup AYDEMİR[3], Canan Aksu CANBAY[4*]
[1] Rare Earth Elements Application and Research Center (MUNTEAM), Munzur University, 62000, Tunceli/TURKEY
[2] Department of Mechanical Engineering, Faculty of Engineering, Mersin University, Mersin, TURKEY
[3,4] Physics Department, Faculty of Science, Firat University, Elazig/TURKEY
[*4] caksu@firat.edu.tr

(Geliş/Received: 23/02/2024; Kabul/Accepted: 26/07/2024)

Abstract: The work presented in this paper reports the shape memory effect characteristics of a CuAlFe high-temperature shape memory alloy (HTSMA) with a new composition and new martensitic transformation temperatures. In this context, casting via a vacuum arc melter produced the Cu-rich ternary CuAlFe high-temperature shape memory alloy (HTSMA). Both DSC and DTA measurement thermograms showed excellent martensitic phase transformation peaks while heating the alloy up and cooling it back. The forward and reverse martensitic phase transformation peaks at different DSC heating/cooling rates had high thermal stability, and the temperature range of these transformations was found above 100 °C between 220-340 °C circa. Therefore, this classifies the alloy as a high-temperature shape memory alloy. Moreover, the formation of the martensite phases, i.e. the microstructural base mechanism for the shape memory effect of the alloy, was confirmed by X-ray diffraction (XRD) pattern obtained at room temperature using CuKα radiation. The findings of this study can be helpful in the high-temperature shape memory alloy-related application areas, in which areas different shape memory properties are highly demanded.

Key words: High-temperature shape memory alloy, CuAlFe, martensitic transformation, DSC.

CuAlFe Yüksek Sıcaklık Şekil Hafızalı Alaşımın Martensitik Dönüşüm Termodinamiği ve Yapı Analizi

Öz: Bu makalede sunulan çalışma, yeni bir bileşime ve yeni martensitik dönüşüm sıcaklıklarına sahip bir CuAlFe yüksek sıcaklık şekil hafızalı alaşımın (YSŞHA) şekil hafıza etkisi özelliklerini rapor etmektedir. Bu kapsamda, bakırca zengin üçlü CuAlFe yüksek sıcaklık şekil hafızalı alaşımı (YSŞHA) vakumlu bir ark eriticide dökümü yapılarak üretildi. Hem DSC hem de DTA ölçüm termogramları, alaşımın ısıtılması ve akabinde soğutulması sırasında mükemmel martensitik faz dönüşüm pikleri gösterdi. Farklı DSC ısıtma/soğutma hızlarında ileri ve ters martensitik dönüşüm piklerinin yüksek ısıl kararlılığa sahip olduğu ve bu dönüşümlerin sıcaklık aralığı 100 °C'nin üzerinde yaklaşık 220-340 °C arasında oluştuğu görüldü. Bundan dolayı alaşım yüksek sıcaklıkta şekil hafızalı alaşım olarak sınıflandırıldı. Ayrıca, martensit fazlarının oluşumu, yani alaşımın şekil hafıza etkisine yönelik mikroyapısal temel mekanizma, CuKa radyasyonu kullanılarak oda sıcaklığında elde edilen X-ışını kırınımı (XRD) deseni ile doğrulandı. Bu çalışmanın bulguları, farklı şekil hafızalı özelliklerin oldukça talep edildiği yüksek sıcaklık şekil hafızalı alaşımlarla ilgili uygulama alanlarında faydalı olabilir.

Anahtar kelimeler: Yüksek sıcaklık şekil hafızalı alaşım, CuAlFe, martensitik dönüşüm, DSC.

1. Introduction

Nowadays, high-temperature shape memory alloys (HTSMAs), as being valuable functional smart materials, with varied properties such as different martensitic transformation temperatures, hysteresis gap, mechanical or other properties are highly demanded in applications utilizing HTSMAs such as automotive, manufacturing, energy exploration, or aero-space [1]. Since the history of studies on shape memory alloys (SMAs) started in the mid of last century [2] due to their unique and functional shape memory effect (SME) and superelasticity (SE) properties, after then HTSMA studies [1,3,4] have started, too.

Among HTSMAs suitable for high-temperature applications [5], high-cost NiTi-based SMAs or HTSMAs [1,3,5–7] have the best thermomechanical shape memory properties. Thus, they are commercially the most preferred ones. NiTiZr and NiTiHf HTSMAs are relatively cheaper than other NiTi-based or Ti-based HTSMAs, but copper-based SMAs and HTSMAs are nearly ten times cheaper than NiTi-based ones. Therefore, studies on

* Sorumlu yazar: caksu@firat.edu.tr. Yazarların ORCID Numarası: [1] 0000-0002-6947-7590, [2] 0000-0003-4255-0564, [4] 0000-0002-5151-4576

copper-based SMAs and HTSMAs are continuously carried out to improve or alter these alloys' SE and SME or other properties to enable their use as alternatives to NiTi-based ones.

The shape change mechanism of SMAs based on their reversible martensitic transformation occurs fundamentally by change of SMAs temperature. The low temperature martensite phase with low symmetry chnges to high temperature austenite phase with high symmetry by increase of temperature or heat intake and this transformation from martensite to austenite is called as reverse transformation. Conversely, when the temperature goes down then austenite converts to martensite and it is called as forward transformation. Martensitic transformation in SMAs occurs isostatically and atomically non-diffusional (atoms move cooperatively and theoretically they do not displace further than atomic lattice parameter or inter-atomic distance) by the effect of internal stresses which are generated by heat intake or release from SMAs. Mostly the austenite unit cell is a cubic phase and for example it transforms to a monoclinic martensite, then a macroscopic shape change can be seen as a sum of all these transformations. This is called as shape memory effect (SME) [8]. The crystallographic SME mechanism of copper-based SMAs is based on a martensitic phase transformation from an austenite (parent) phase with high symmetry cubic β-phase (DO_3 or $L2_1$) to a martensite (product) phase with lower symmetry monoclinic (β') or orthorhombic (γ') or a mixture (β'+ γ') martensite structure [9]. This structural SME mechanism is susceptible to the alloying composition, thermal treatment, and stress levels of these SMAs. Even a slight variation in the alloy composition can substantially alter the SME characteristics. For this reason i.e. in order to improve or modify shape memory properties and/or reduce the grain size for enhancement of mechanical properties, adding one or more extra elements such as Ti, Mn, Ni, Fe, Co, Be, Sn, Zn, etc., called grain refining elements, to the binary copper-based SMAs is a practical and prevalent method used to improve or modify shape memory parameters of copper-based SMAs.

Among Cu-based SMAs, binary CuAl-based HTSMAs exhibit martensitic transformation (operation) in higher temperature ranges than the other Cu-based ones [10] and also better microstructural stability [1] and electric and thermal conductivity [11]. Especially the foremost CuAlNi (or -based) and the other CuAlMnNi, CuAlMnTi, CuAlNb, CuAlBe, CuAlTa, and CuAlFeMn HTSMAs [1,9,10,12–14] are the most outstanding CuAl-based (or Cu-based) HTSMAs. Ternary CuAlFe HTSMAs with excellent SME [13,15,16] have also distinguished in the last decade. For example, in one of these works, the Cu-xAl-4Fe (x = 11, 13, 15wt%) alloys were studied and it was reported that the alloy is very sensitive to Al fraction and the M_s temperature decreased substantially by the increase of Al content (from 11wt% to 15wt% Al, it decreased by up to 217 °C), also the microstructure presented sub-eutectic to hyper-eutectic characteristics with the rise in Al content, and while the shape memory recovery rates of the 13 and 15wt% Al alloys were determined as 100%, the recovery rate of 11wt% Al alloy was determined only as 22.6%, but the lowest ductility (or the highest brittleness) was found in the 15wt% Al alloy. In another work [15], the $Cu_{84-x}Al_{11+x}Fe_5$ (x = 0, 1, 2) alloys were investigated and it was stated that the β1' and γ1' martensites form together for the Al content of 11 and 12 wt%, but in the case of 12 wt% of Al content γ1' forms dominantly, and the ductility of alloy gradually increases with the decrease of Al content. In the other work, the influence of Al content (in the range of 10-13 wt %) on the two groups of Cu-Al-Fe alloys, one with only varying Al contents and the other with only varying Fe contents, were studied and it was observed that the transformation temperatures reduced with increase of Al, but they increased with increase of Fe content, and again the dominancy changing from β1' to γ1' martensite was observed through going from low to high Al content. However, studies on these HTSMAs are still very few, and their thermodynamic transformation parameters were not adequately investigated. Also, not many options for different transformation temperatures have been reported. Therefore, a CuAlFe HTSMA with different transformation temperatures was produced in this study, and its thermodynamic aspects were investigated.

2. Experimental Details

The ternary CuAlFe HTSMA was produced by the following steps (as shown in Figure 1): 1- The high %99.9-purity of Cu, Al, and Fe metal elements powders were mixed. 2- The tablet-like pellets was formed from the powder-mixture by applying pressure. 3- Ingot alloy was cast by melting the pellets in a vacuum arc melter. 4- The ingot alloy pieces proper for test samples were cut and for one (1) h the samples were homogenized at 900 °C and quenched immediately in iced-brine water to form martensitic structure mechanism in the HTSMA to have SME property. In order to observe and analyze the heat-induced SME behaviour of the HTSMA, a Shimadzu-60A label DSC equipment was used at varied heating/cooling rates between 10 - 25 °C/min and running between room temperature and 380 °C under a constant flow rate of 100 ml/min of inert (argon) gas. For high-temperature region behaviours of the HTSMA, a Shimadzu DTG-60AH model DTA equipment was used under the same inert gas flow at 25 °C/min of heating/cooling rate between room temperature and 900 °C. The XRD pattern of the produced CuAlFe HTSMA was obtained in the room condition using CuKα wavelength rays in a Rigaku Miniflex 600 model X-ray diffractometer to determine the martensite structures of the SME mechanism formed in the HTSMA matrix.

Using the SEM-Hitachi SU3500 instrument at room temperature, the EDS test was performed to detect the alloying composition of the CuAlFe HTSMA.

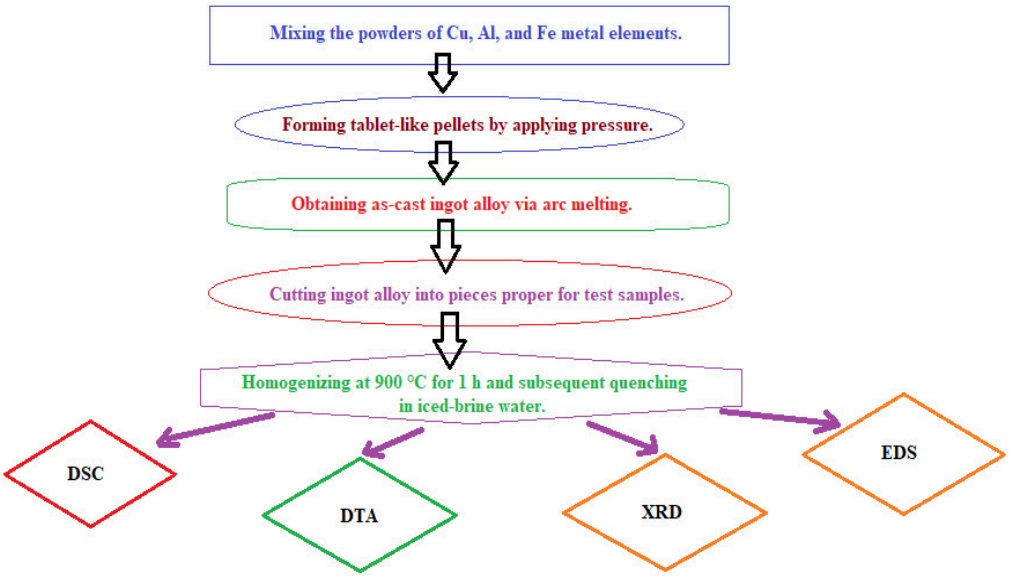

Figure 1. The flow diagram showing the production and characterization steps of the ternary CuAlFe HTSMA.

3. Results and Discussion

The XRD pattern of the fabricated CuAlFe HTSMA is given in Figure 2 and displays the peaks indicating the formed martensite and other phases in the alloy at room temperature. The observed main or most powerful intensity peak is a monoclinic β'1 type martensite with an orientation of (128) Miller indices. This main peak and the other smaller monoclic β'1(18R) and hexagonal γ'1(2H) martensite peaks [9,13,15–17] mean that a crystallographic structure mechanism for a shape memory effect property of the CuAlFe alloy is formed in the alloy texture by the effect of rapid cooling (quenching) right at the end of homogenization. Lastly, there a small copper-rich α-phase peak is also seen formed on this XRD pattern. It is seen that both β'1 and γ'1 types of martensites, with volumetric dominancy of β'1 martensite over γ'1 martensite, were formed together contextured in the alloy texture and the formation of which martensite types and dominancy over each other depend on the average valence electron concentration per atom ratio (e/a) parameter value of the alloy. This e/a parameter value calculated for the CuAlFe alloy is to be given ahead in the EDS result section.

By using the XRD data of the main martensite peak, the crystallite size of the CuAlFe alloy was also calculated by using the Debye-Scherrer formula [9] as given below;

$$D = \frac{0.9\lambda}{B_{\frac{1}{2}} \cos\theta} \quad (1)$$

Where λ stands for the wavelength (CuKα radiation, λ= 0.15406 nm) used for X-ray diffraction, $B_{1/2}$ refers to the full width at half maximum (FWHM) value of the main intensity martensite peak, and θ refers to the Bragg diffraction angle of this peak. So, at the 2θ angle of 44.418° with a corresponding FWHM value of 0.953, the crystallite size D value of the CuAlFe HTSMA was calculated as 9.01 nm. This value was found as similar to 9.29 nm found for the 73.23Cu-21.93Al-3.36Fe1.48Mn (at.%) alloy aged and quenched in boiling water [18], close to 15.61 nm found for the quinary Cu-24.08Al-2.23Fe-1.34Co-0.97Ti (at%) alloy [19], lower than 20.02 nm found for Cu-22.78Al-2.59Fe-2.44Mn (at%) [9], and than 21.12 nm found for Cu-23.08Al-0.5Mn (at%) [20], previously. When these reported D values of the alloys with Fe contents are compared, it seems that the crystallite size decreased with increase of Fe content.

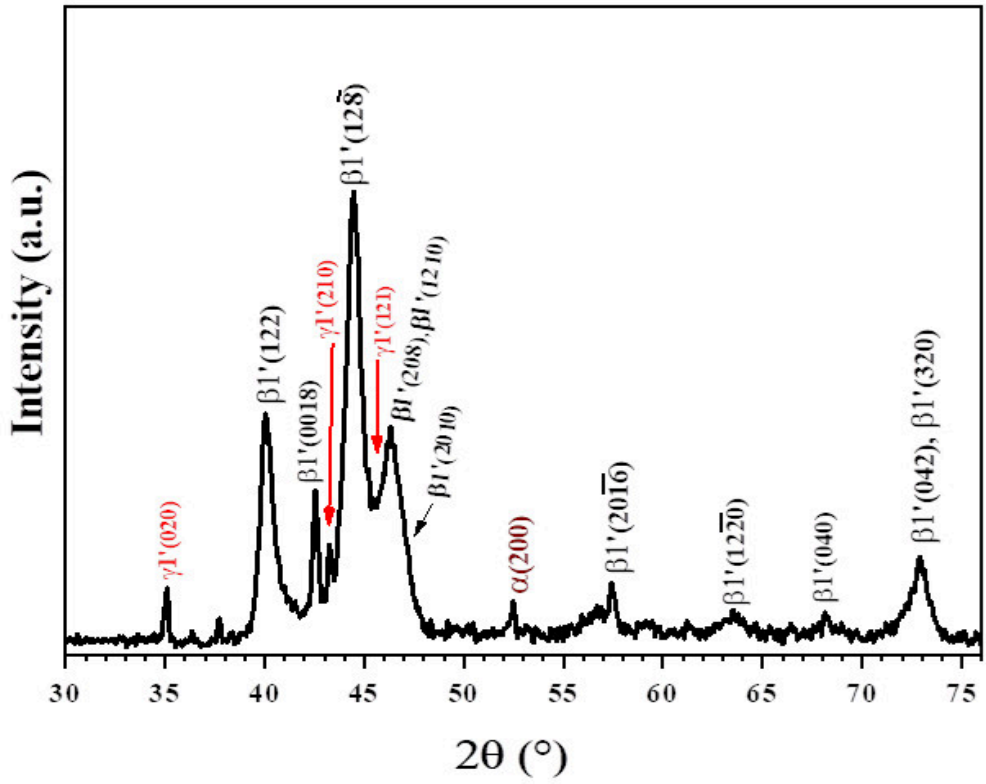

Figure 2. The XRD pattern of the ternary CuAlFe HTSMA at room temperature.

The EDS pattern of the ternary CuAlFe HTSMA is given in Figure 3. This EDS test detects the alloying composition of the produced CuAlFe HTSMA as $_{72.28}$Cu-$_{23.71}$Al-$_{4.01}$Fe (at.%).

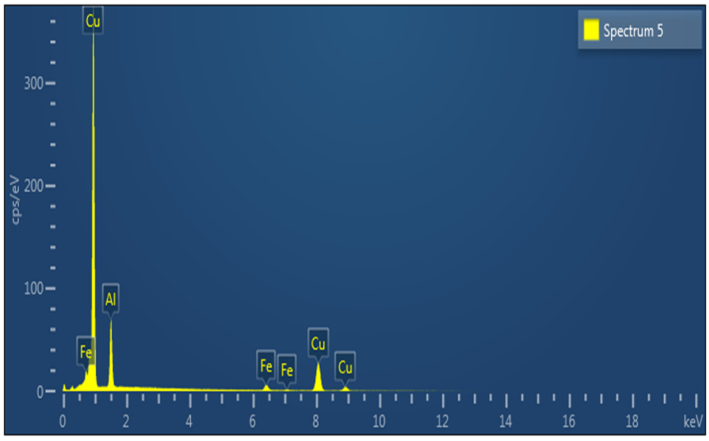

Figure 3. The EDS test pattern of the produced CuAlFe HTSMA.

By using atomic at.% percentages (fractions) of the constituent elements of the detected alloy's composition in the formula [9] given as $e/a=\Sigma f_i.v_i$, and in this formula: f refers to the atomic fractions of the alloying elements and v stands for the corresponding valence electron numbers of these elements. In this way, the e/a ratio of the average electron concentration ratio (e/a) of the CuAlFe alloy was 1.51. The e/a ratio of CuAlFe alloy is found between the e/a ratio range of 1.45-1.51, which is a theoretical condition for Cu-based alloys to have a shape memory effect [8,9]. Moreover, Cu-based SMAs with e/a ratios in this range can have two different martensite forms (β1′ and γ1′) together, and β1′ martensite gains dominancy over γ1′ martensite by going from 1.51 to 1.45.

The XRD result given above confirmed the formation of these two martensite phases in the CuAlFe alloy predicted by the alloy's e/a ratio of the alloy.

The DSC curves of the CuAlFe HTSMA obtained by DSC cycles run at different 15-30 °C/min heating/cooling rates as multi-curves in Figure 4. On each one of these curves, while the downward endothermic peaks indicate the reverse martensite-to-austenite (M→A) phase transformations, the upward exothermic peaks indicate the forward austenite-to-martensite (A→M) phase transformations occurred upon heating and then cooling the DSC test sample piece of CuAlFe HTSMA, respectively [9,11,21].

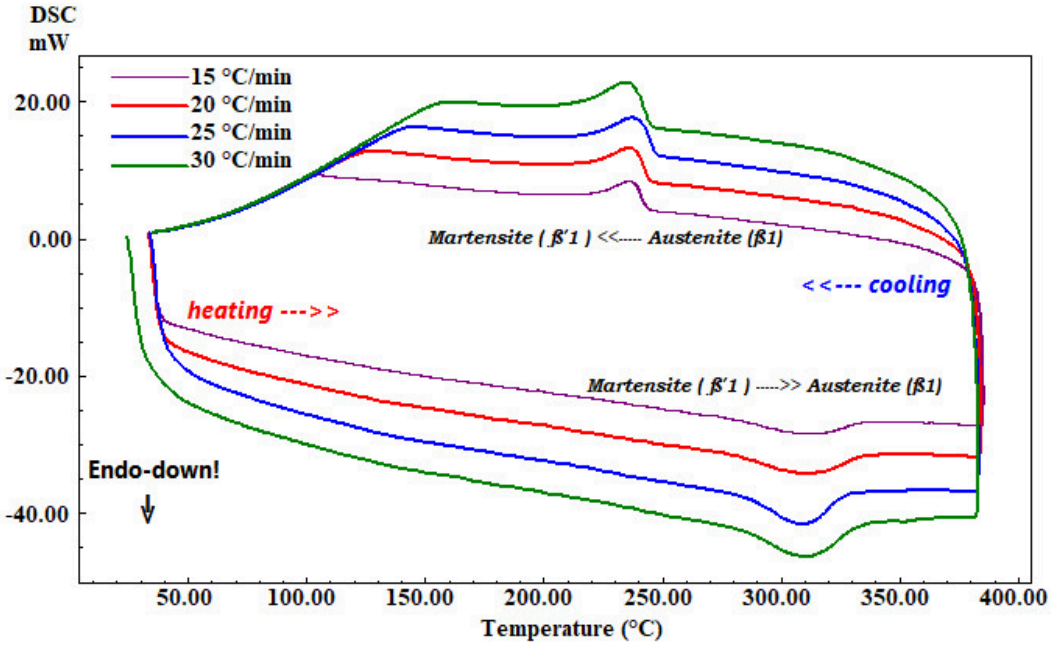

Figure 4. The cycling DSC, heating/cooling curves, taken at different 15, 20, 25 and 30 °C/min heating/cooling rates, show the reverse martensite to austenite (M→A) transformation peaks on heating fragments of these curves and the forward austenite to martensite (A→M) transformation peaks on cooling fragments of these curves.

The characteristic operation (martensitic transformation) temperatures and other thermokinetic parameter values of the CuAlFe HTSMA determined from the DSC peak analyses data and based calculations were all presented in Table 1. In this table, values of the thermal equilibrium temperature (T_0) parameter; at this temperature, there is no driving force for a martensitic transformation to occur because no difference between the Gibbs (chemical) free energies of austenite and martensite phases exists at an equilibrium temperature, were determined by $T_0=(A_f+M_s)\times 0.5$ formula [9,11]. Also, the entropy change (ΔS) parameter value for each M→A transformation reaction was determined by using the enthalpy change (ΔH) values in $\Delta S_{M\rightarrow A}=\Delta H_{M\rightarrow A}/T_0$ formula [9,11]. As a result, the high enthalpy change amounts of these martensitic transformations, reached its maximum 12.03 J/g value at the 30 °C/min heating/cooling rate, indicate the potent suitable shape memory effect property of the CuAlFe HTSMA.

Another important reaction kinetic parameter is activation energy (E_a), which is proper for a martensitic transformation; it plays a critical role in the occurrence of martensitic phase transformations and determines the crystallization behaviour of the alloy. Also, to to determine this energy parameter is important in the industrial productions and applications of shape memory alloys. Here, the formula of Kissinger [9,22] relevant for martensitic transformation was used to compute the E_a value of the M→A transformation of CuAlFe alloy;

$$\frac{d\left[ln\left(\frac{\phi}{T_m^2}\right)\right]}{d\left(\frac{1}{T_m}\right)} = -\frac{E_a}{R} \qquad (2)$$

Table 1. The characteristic martensitic transformation temperatures and other related thermodynamic parameters of the fabricated CuAlFe HTSMA.

Heating/cooling rate (°C/min)	A_s (°C)	A_f (°C)	A_{max} (°C)	M_s (°C)	M_f (°C)	A_s-M_f (°C)	T_0 (°C)	$\Delta H_{M\rightarrow A}$ (J/g)	$\Delta S_{M\rightarrow A}$ (J/g°C)
15	286.65	331.97	308.10	243.72	221.04	65.61	287.85	9.90	0.0344
20	283.80	334.90	309.97	244.88	217.87	65.93	289.89	11.37	0.0392
25	288.14	326.56	310.03	247.92	217.54	70.60	287.24	11.43	0.0398
30	285.61	333.01	311.01	245.37	214.80	70.81	289.19	12.03	0.0416
Avg.	286.05	331.61	309.78	245.47	217.81	68.24	288.54	11.18	0.0388

Where T_m refers to the peak maximum temperature (A_{max}) of M→A transformation, ϕ stands for heating/cooling rate, and R is (=8.314 J/mol.K) the universal gas constant. A plot showing the activation energy change of the reverse M→A transformation of the CuAlFe HTSMA was drawn and presented in Figure 5. By taking linear fitting on this plot, obtaining its slope value (seen in the inset fitting dataset in this graphic), and substituting it instead of the left term in Eq.2, the activation energy for the reverse martensitic phase transition reaction of the CuAlFe HTSMA can be found. Thus, the E_a activation energy value of the CuAlFe HTSMA was 651.28 kJ/mol. This value was found close to those reported in some previous works [9,23].

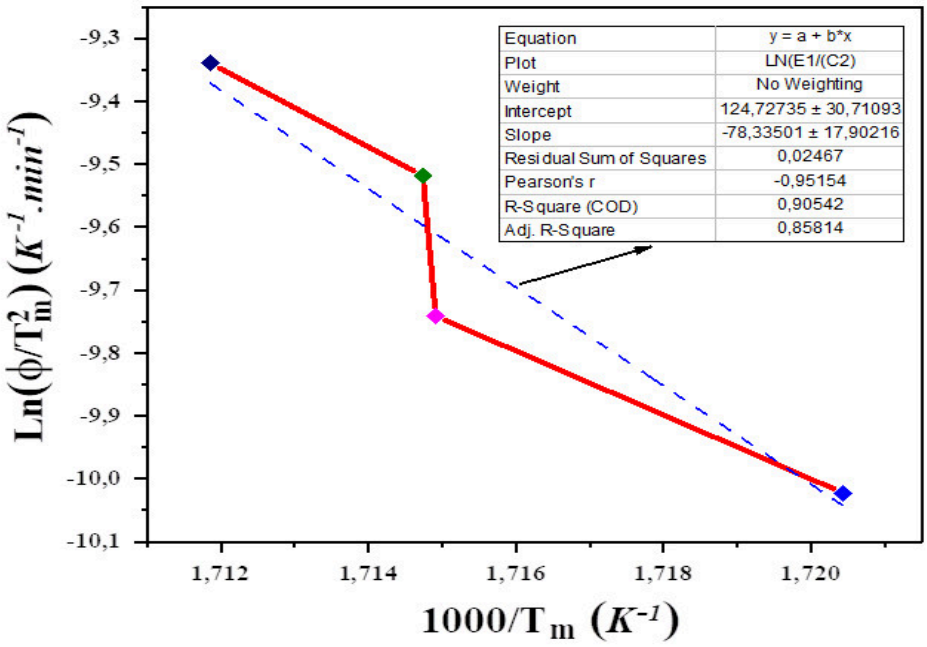

Figure 5. Activation energy change plot of the CuAlFe HTSMA with linear fitting line and inset dataset.

DTA high-temperature thermogram curve of the alloy obtained at a single 25 °C/min heating/cooling rate is given in Figure 6. On the up fragment of this DTA curve representing the cooling of the CuAlFe alloy sample back to room temperature, there is a series of multiple sequential phase transition steps of A2→B2→B1(DO_3 or $L2_1$)→β'1 as commonly seen in the other Cu-based SMAs and HTSMAs [8,9,11,24–26]. The DTA curve of the CuAlFe alloy also shows its forward and reverse martensite transformation peaks. The sharp and deep eutectoid point peak indicates how well the CuAlFe HTSMA is alloyed.

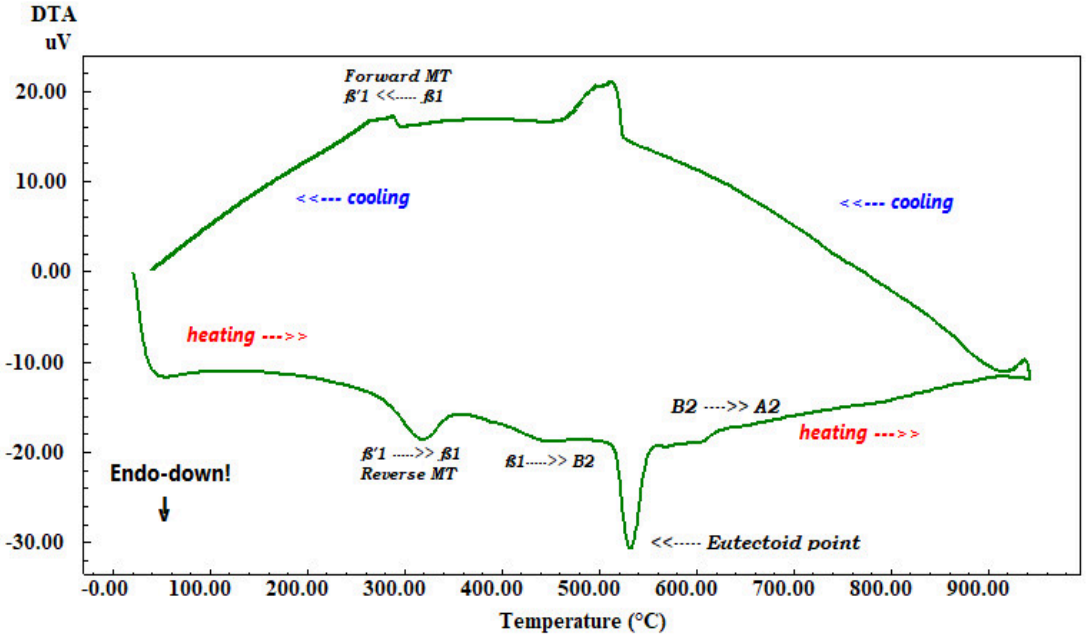

Figure 6. The cycling DTA heating/cooling curve of the fabricated CuAlFe HTSMA taken at a single 25 °C/min heating/cooling rate shows the multiple-phase transition chain on heating as follows: martensite (β1′) →austenite (β1, L21) → B2 (metastable cubic) → precipitating → eutectoid dissolution → B2 (ordered cubic) →A2 (disordered cubic).

4. Conclusions

The CuAlFe HTSMA was produced successfully by arc melting method. The homogenization and quenching led martensitic structures to be formed in the alloy to have a shape memory property. The XRD pattern of the alloy confirmed the formed martensite structures in the alloy. Also, it confirmed the supportive prediction of the formation of these martensite structures made upon the alloy's calculated average valence electron concentration ratio. The DSC and DTA results showed the powerful forward and reverse martensitic transformations that happened upon heating and cooling the alloy. The determined operation temperatures of the alloy showed that the alloy is a high-temperature shape memory alloy and they are different than those in the literature. Also, the enthalpy and entropy change amounts were found as the highest reached ever in the literature, showing the powerful shape memory capacity of the produced alloy. The determined high activation energy of the reverse transformation of the alloy is related to its polycrystallinity and small crystallite size which enlarged the total surface area of martensite crystallites to transform to austenite thus increase the activation energy needed for this transformation. The determined crystallite size of the alloy was found mostly smaller than those reported in the literature, due to the high Fe content use. All findings of this study indicate that the fabricated CuAlFe HTSMA with new martensitic transformation temperatures may be useful in HTSMA-related smart material applications.

Acknowledgments

This research work is a part of thesis works of Yakup AYDEMİR mastering in general physics in Physics Department, Science Faculty, Firat University. Firat University Scientific Research Projects (FUBAP) financially supports this research work: FF.23.17 project number.

References

[1] Ma J, Karaman I, Noebe RD. High temperature shape memory alloys. International Materials Reviews 2010;55:257–315.
[2] Kauffman GB. The Story of Nitinol: The Serendipitous Discovery of the Memory Metal and Its Applications. The Chemical Educator 1997;2:1–21.
[3] Firstov GS, Van Humbeeck J, Koval YN. High-temperature shape memory alloys. Materials Science and Engineering: A 2004;378:2–10.
[4] Duerig TW, Albrecht J, Gessinger GH. A Shape-Memory Alloy for High-Temperature Applications. JOM 1982;34:14–20.

[5] Van Humbeeck J. Shape memory alloys with high transformation temperatures. Mater Res Bull 2012;47:2966–8.
[6] Hite N, Sharar DJ, Trehern W, Umale T, Atli KC, Wilson AA, et al. NiTiHf shape memory alloys as phase change thermal storage materials.
[7] Ley NA, Wheeler RW, Benafan O, Young ML. Characterization of Thermomechanically Processed High-Temperature Ni-Lean NiTi–20 at.% Hf Shape Memory Wires. Shape Memory and Superelasticity 2019;5.
[8] Otsuka K, Wayman CM. Shape memory materials. Cambridge University Press; 1999.
[9] Canbay CA, Karaduman O, Ünlü N, Baiz SA, Özkul İ. Heat treatment and quenching media effects on the thermodynamical, thermoelastical and structural characteristics of a new Cu-based quaternary shape memory alloy. Compos B Eng 2019;174:106940.
[10] Mazzer EM, Da Silva MR, Gargarella P. Revisiting Cu-based shape memory alloys: Recent developments and new perspectives. J Mater Res 2022;37:162–82.
[11] Canbay CA, Karaduman O. The photo response properties of shape memory alloy thin film based photodiode. J Mol Struct 2021;1235:130263.
[12] Canbay CA, Karaduman O, Özkul İ. Investigation of varied quenching media effects on the thermodynamical and structural features of a thermally aged CuAlFeMn HTSMA. Physica B Condens Matter 2019;557:117–25.
[13] Wang H, Huang J, Chen S, Yuan X, Zhu J, Xu D, et al. Microstructure and shape memory properties of Cu-Al-Fe alloys with different Al contents made by additive manufacturing technology. Mater Res Express 2022;9:095701.
[14] Najah Saud Al-Humairi S. Cu-Based Shape Memory Alloys: Modified Structures and Their Related Properties. Recent Advancements in the Metallurgical Engineering and Electrodeposition, IntechOpen; 2020, p. 25.
[15] Yang S, Su Y, Wang C, Liu X. Microstructure and properties of Cu-Al-Fe high-temperature shape memory alloys. Mater Sci Eng B Solid State Mater Adv Technol 2014;185:67–73.
[16] Raju TN, Sampath V. Influence of aluminium and iron contents on the transformation temperatures of Cu-Al-Fe shape memory alloys. Transactions of the Indian Institute of Metals 2011;64:165–8.
[17] Saud SN, Hamzah E, Abubakar T, Bakhsheshi-Rad HR. Thermal aging behavior in Cu-Al-Ni-xCo shape memory alloys. J Therm Anal Calorim 2015;119:1273–84.
[18] Canbay CA, Karaduman O, Özkul İ, Ünlü N. Modifying Thermal and Structural Characteristics of CuAlFeMn Shape Memory Alloy and a Hypothetical Analysis to Optimize Surface-Diffusion Annealing Temperature. J Mater Eng Perform 2020;29:7993–8005.
[19] Karaduman O, Özkul I, Altın S, Altın E, Bağlayan, Canbay CA. New Cu-Al based quaternary and quinary high temperature shape memory alloy composition systems. AIP Conf Proc, vol. 2042, American Institute of Physics Inc.; 2018.
[20] Karaduman O, Aksu Canbay C, Özkul İ, Aziz Baiz S,, Ünlü N. Production and Characterization of Ternary Heusler Shape Memory Alloy with A New Composition. Journal of Materials and Electronic Devices 2018;1:9–16.
[21] Canbay CA, Karaduman O, Özkul İ. Lagging temperature problem in DTA/DSC measurement on investigation of NiTi SMA. Journal of Materials Science: Materials in Electronics 2020;31:13284–91.
[22] Kissinger HE. Reaction Kinetics in Differential Thermal Analysis. Anal Chem 1957;29:1702–6.
[23] Canbay CA, Karaduman O, Ünlü N, Özkul İ, Çiçek MA. Energetic Behavior Study in Phase Transformations of High Temperature Cu–Al–X (X: Mn, Te, Sn, Hf) Shape Memory Alloys. Transactions of the Indian Institute of Metals 2021.
[24] Prado MO, Decorte PM, Lovey F. Martensitic transformation in Cu-Mn-Al alloys. Scripta Metallurgica et Materialia 1995;33.
[25] Chentouf SM, Bouabdallah M, Gachon JC, Patoor E, Sari A. Microstructural and thermodynamic study of hypoeutectoidal Cu-Al-Ni shape memory alloys. J Alloys Compd 2009;470:507–14.
[26] Grgurić TH, Manasijević D, Kožuh S, Ivanić I, Anžel I, Kosec B, et al. The effect of the processing parameters on the martensitic transformation of Cu-Al-Mn shape memory alloy. J Alloys Compd 2018;765:664–76.